PROCEEDINGS OF SCIENCE

Extracting the scalar dynamical polarizabilities from real Compton scattering data

P. Pedroni*
INFN, Sezione di Pavia - Pavia, Italy
E-mail: paolo.pedroni@pv.infn.it

B. Pasquini[ab]
[a]*Dipartimento di Fisica, Università degli studi di Pavia - Pavia, Italy*
[b]*INFN, Sezione di Pavia - Pavia, Italy*
E-mail: barbara.pasquini@unipv.it

S. Sconfietti[ab]
[a]*Dipartimento di Fisica, Università degli studi di Pavia - Pavia, Italy*
[b] *INFN, Sezione di Pavia - Pavia, Italy*
E-mail: stefano.sconfietti@pv.infn.it

We discuss the advantages of a statistical technique, based on the simplex minimization and on the parametric bootstrap, with respect to the standard χ^2-minimization method. We present the application of this technique for the extraction of the proton scalar dipole dynamical polarizabilities from real Compton scattering data. In particular, we discuss how this technique is able to provide realistic probability distributions of the fitted parameters, with no a-priori assumptions on their shape, and to include the systematic errors in the minimization procedure in a straightforward way.

23rd International Spin Physics Symposium - SPIN2018 -
10-14 September, 2018
Ferrara, Italy

*Speaker.

https://pos.sissa.it/

PoS(SPIN2018)122

1. Polarizabilities in the proton

Real Compton scattering (RCS) gives a clean experimental access to the nucleon polarizabilities, that are elementary structure constants such as its size, shape, and magnetic moment. In RCS at low energies, the incoming real photon plays the role of an applied quasi-static electromagnetic field that deforms the charge and magnetization densities of the nucleon. These induced polarizations can be measured through the energy and angular distribution of the RCS process and are parametrized in terms of nucleon dipole and higher-order static polarizabilities. Taking into account the spatial and time dependence of the applied electromagnetic field, one observes internal relaxation mechanisms, resonances and particle production, which make the polarizabilities depending on the energy: this dependence is subsumed in the definition of dynamical polarizabilities, that parametrize the response of the internal degrees of freedom of a composite object to an external, real-photon field of arbitrary energy [1, 2, 3].
The definition of dynamical polarizabilities is given in terms of the multipole amplitudes $f^{l\pm}_{TT'}$, which correspond to the transition $Tl \to T'l'$, with $T,T' = E,M$ and $\pm$ giving the total angular momentum $j = l \pm 1/2$. In particular, for the scalar dipole electric $\alpha_{E1}(\omega)$ and magnetic $\beta_{M1}(\omega)$ dynamical polarizabilities one has the following combination of the $l = 1$ multipoles

$$\alpha_{E1}(\omega) \equiv \frac{2f^{1+}_{EE}(\omega)+f^{1-}_{EE}(\omega)}{\omega^2}, \qquad \beta_{M1}(\omega) \equiv \frac{2f^{1+}_{MM}(\omega)+f^{1-}_{MM}(\omega)}{\omega^2}, \tag{1.1}$$

where ω is the center of mass (c.m.) photon energy.
The extraction of the dynamical polarizabilities from RCS data is quite challenging. In this work we summarize the method proposed in Ref. [4] that allowed us to gain first insights on the scalar dipole dynamical polarizabilities (DDPs) from RCS data.

2. Fitting technique

The scalar DDPs are parameterized as:

$$\alpha_{E1}(\omega) = f_\alpha(\alpha_{E1}, \alpha_{E1,\nu}, \beta_{M1}, \beta_{M1,\nu}) + g_\alpha(\alpha_{E2}, \beta_{M2}, \gamma_i) + h_\alpha(h.t.), \tag{2.1}$$

$$\beta_{M1}(\omega) = f_\beta(\alpha_{E1}, \alpha_{E1,\nu}, \beta_{M1}, \beta_{M1,\nu}) + g_\beta(\alpha_{E2}, \beta_{M2}, \gamma_i) + h_\beta(h.t.). \tag{2.2}$$

In Eqs. (2.1) and (2.2), $f_{\alpha,\beta} + g_{\alpha,\beta}$ correspond to the low-energy expansion (LEX) of the DDPs up to $\mathscr{O}(\omega^5)$. In particular, the functions $f_{\alpha,\beta}$ contain the contribution from the dipole scalar electric (α_{E1}) and magnetic (β_{M1}) polarizabilities as well as from the dispersive polarizabilities $\alpha_{E1,\nu}$ and $\beta_{M1,\nu}$, while $g_{\alpha,\beta}$ depend on the quadrupole electric (α_{E2}) and magnetic (β_{M2}) static polarizabilities, and the static leading- and higher-oder spin polarizabilities γ_i. The functions $h_\alpha(h.t.)$ and $h_\beta(h.t.)$ give the residual energy dependence beyond the LEX.

In our analysis, we use the predictions from fixed-t dispersion relations (DRs) for the higher-order polarizabilities [5, 6, 7], and the experimental values extracted in Ref. [8] for the leading-order static spin polarizabilities. Likewise, we use fixed-t DRs to calculate the functions $h_\alpha(h.t.)$ and $h_\beta(h.t.)$. The functions $f_{\alpha,\beta}(\alpha_{E1}, \alpha_{E1,\nu}, \beta_{M1}, \beta_{M1,\nu})$ are fitted to RCS data and contain four free parameters, i.e. $\alpha_{E1}, \alpha_{E1,\nu}, \beta_{M1}$, and $\beta_{M1,\nu}$. Using the additional constraint from the Baldin sum rule, $\alpha_{E1} + \beta_{M1} = (13.8 \pm 0.4) \cdot 10^{-4}$ fm^3 [9], the number of fit parameters is finally reduced to three.

We used the data set of all the available experimental data for the unpolarized RCS cross section below pion-production threshold, as listed in Ref. [4]. First, we tried to apply the standard χ^2-minimization procedure using the Newton (gradient) method. However, we found that this method does not work due to *i*) high correlation among the fitting parameters and *ii*) low sensitivity of the unpolarized RCS differential cross section to the DDPs coefficients. In particular, it was not possible to achieve the positive-definiteness condition of the covariance matrix.
In order to solve this problem, we combined the geometrical simplex method for the minimization in Minuit [10] and the parametric bootstrap [11], which is a Monte Carlo technique. The basic idea is to approximate the true (and unknown) probability distribution of the single experimental datum with the (known) probability distribution given by the measured value with its statistical error. The only a priori assumption is the choice of the specific probability distribution associated to the experimental point.

Schematically, in the case of gaussian-distributed statistical errors having a common systematic scale-factor uncertainty, the bootstrap sampling can be written as

$$B_{i,j,k} = (1 + \delta_{j,k})(E_i + \gamma_{i,j}\sigma_i), \tag{2.3}$$

where E_i is the experimental value of the differential cross section, with a statistical error σ_i. In Eq. (2.3), the index i runs over the data points, j labels the number of replicas and k indicates different data sub-sets. The number $\gamma_{i,j}$ is distributed according to a standard Gaussian $\mathscr{N}[0,1]$, while $\delta_{j,k}$ follows a box distribution $\mathscr{U}[-\Delta_k, \Delta_k]$, where Δ_k is the published systematic error for each data sub-set or, if more than one source for systematics is present, the product of all the different contributions.
We then use our bootstrapped data $B_{i,j,k}$ for the usual evaluation of χ^2 function, that is minimized with the simplex technique. After every bootstrap cycle, we then obtain a different estimate of the best values of the fitting parameters, that allows us to reconstruct their probability distributions.

Our fitting technique has several advantages:

- the straightforward inclusion of systematical errors without substantial modifications in the definition of the χ^2 function;
- the realistic probability distributions for the fitted parameters is obtained without any a priori assumption;
- the error propagation procedure is performed without using any approximated formulas;
- the probability distributions of every functions depending on the fitted parameters (such as the DDPs or the differential cross section) are evaluated with the automatical inclusion of all their correlation terms.

In Fig. 1 we show our fit results for the DDPs as function of the photon c.m. energy, with the 68% and 95% confidence level (*CL*) bands in comparison with the predictions of DRs [2].

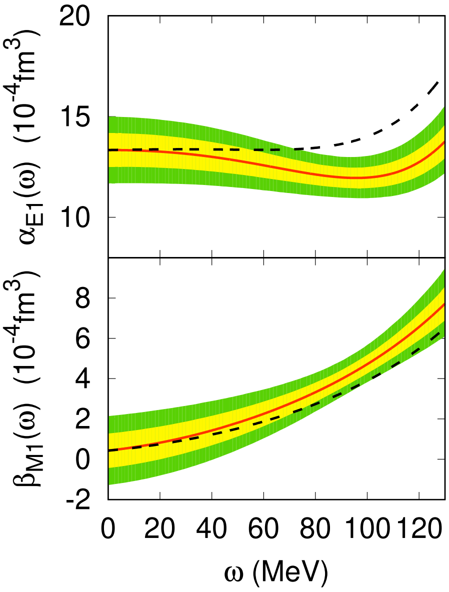

Figure 1: Results from the fit of the scalar DDPs as function of the c.m. photon energy ω: $\alpha_{E1}(\omega)$ on the top and $\beta_{M1}(\omega)$ on the bottom. The 68% (yellow) and 95% (green) *CL* areas include all the correlations between the parameters. The dashed lines are the predictions from DRs [2].

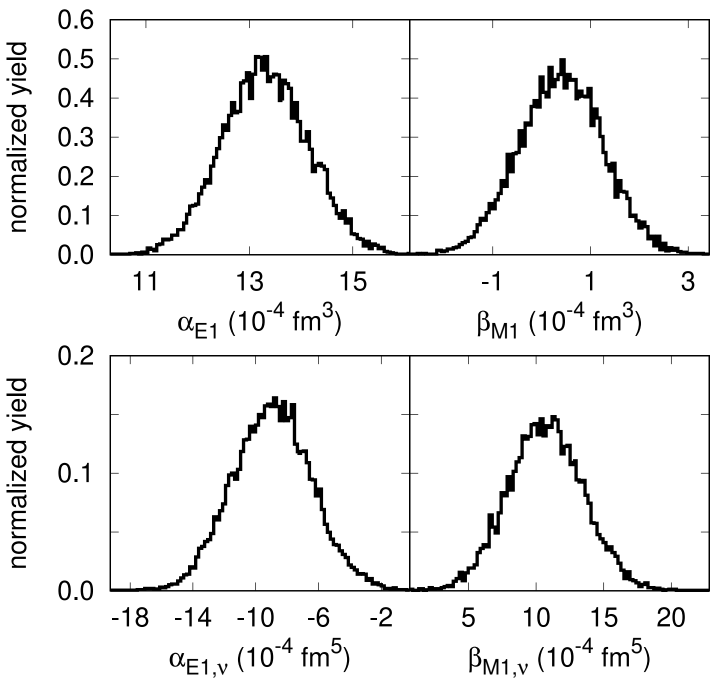

Figure 2: Probability distributions for the fitted parameters of the scalar DDPs.

In Fig. 2 we show the probability distributions for the fitted parameters.
It is noteworthy to remark that, in general, the distribution of the minimal values of the χ^2 function evaluated by our technique is not distributed like a χ^2 distribution, i. e. it is not the sum of the squares of independent standard Gaussian random variables. This a consequence of the Monte Carlo sampling of Eq. (2.3) and reflects one of the main effects due to the inclusion of systematical errors, which correlate all point within a single subset.

As an example, we show in Fig. 3 the reconstructed probability distribution of the minimum values of the χ^2 function (χ^2_{min}) after each bootstrap cycle in the case of a two-parameter fit, i.e. α_{E1} and β_{M1}. The modification on the shape of this distribution after the inclusion of systematical errors is clearly visible.

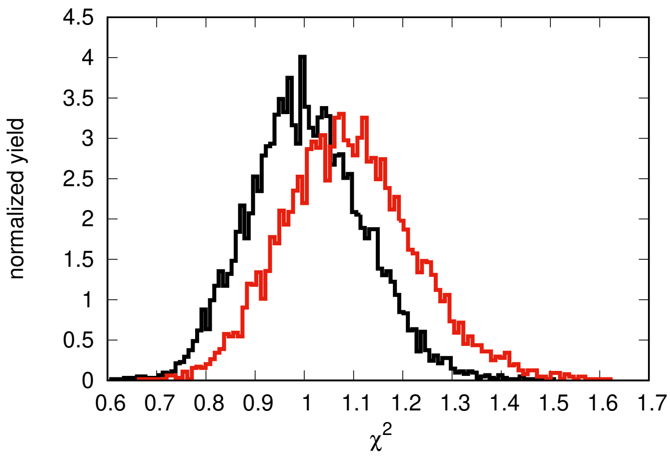

Figure 3: Probability distributions for the χ^2_{min} variable obtained by our fitting technique with a two-parameter fit. The usual χ^2 distribution is obtained when only statistical errors are taken into account (black line), while a different distribution (red line) is obtained when also systematic uncertainties are included.

3. Conclusions

We discussed a parametric bootstrap technique to analyze proton RCS data for the extraction of the DDPs. We outlined several advantages of this technique, and refer to a forthcoming work [12] for a more comprehensive description of the statistical features of the method. This fitting procedure has never been applied so-far to analyze RCS data, and we plan to use it for a re-evaluation of the proton scalar dipole static polarizabilities [12] from the existing RCS data, using fixed-t DRs for the theoretical framework.

References

[1] H. W. Griesshammer and T. R. Hemmert, *Dispersion effects in nucleon polarizabilities*, *Phys. Rev. C* **65** (2002) 045207.

[2] R. P. Hildebrandt, H. W. Griesshammer, T. R. Hemmert and B. Pasquini, *Signatures of chiral dynamics in low-energy compton scattering off the nucleon*, *Eur. Phys. J. A* **20** (2004) 293.

[3] V. Lensky, J. McGovern and V. Pascalutsa, *Predictions of covariant chiral perturbation theory for nucleon polarisabilities and polarised Compton scattering*, *Eur. Phys. J. C* **75** (2015) 604.

[4] B. Pasquini, P. Pedroni and S. Sconfietti, *First extraction of the scalar proton dynamical polarizabilities from real compton scattering data*, *Phys. Rev. C* **98** (2018) 015204.

[5] B. Pasquini, D. Drechsel and M. Vanderhaeghen, *Proton spin polarizabilities from polarized Compton scattering*, *Phys. Rev. C* **76** (2007) 015203.

[6] D. Drechsel, M. Gorchtein, B. Pasquini and M. Vanderhaeghen, *Fixed t subtracted dispersion relations for Compton Scattering off the nucleon*, *Phys. Rev. C* **61** (1999) 015204.

[7] B. R. Holstein, D. Drechsel, B. Pasquini and M. Vanderhaeghen, *Higher order polarizabilities of the proton*, *Phys. Rev. C* **61** (2000) 034316.

[8] A2 collaboration, P. P. Martel et al., *Measurements of Double-Polarized Compton Scattering Asymmetries and Extraction of the Proton Spin Polarizabilities*, *Phys. Rev. Lett.* **114** (2015) 112501.

[9] PARTICLE DATA GROUP collaboration, C. Patrignani et al., *Review of Particle Physics*, *Chin. Phys. C* **40** (2016) 100001.

[10] F. James and M. Roos, *Minuit: A System for Function Minimization and Analysis of the Parameter Errors and Correlations*, *Comput. Phys. Commun.* **10** (1975) 343.

[11] A. C. Davidson and D. V. Hinkley, *Bootstrap Methods and their Application*. Cambridge University Press, 1997.

[12] P. Pedroni, S. Sconfietti et al., *in preparation*.